




Canopy structure and topography jointly constrain the microclimate of human-modified tropical landscapes

Tommaso Jucker^{1,2}  | Stephen R. Hardwick³ | Sabine Both^{4,5}  | Dafydd M.O. Elias^{6,7} | Robert M. Ewers⁸ | David T. Milodowski⁹ | Tom Swinfield¹ | David A. Coomes¹ 

¹Forest Ecology and Conservation group, Department of Plant Sciences, University of Cambridge, Cambridge, UK

²CSIRO Land and Water, Floreat, WA, Australia

³Blackett Laboratory, Department of Physics, Imperial College London, London, UK

⁴School of Environmental and Rural Science, University of New England, Armidale, NSW, Australia

⁵Institute of Biological and Environmental Sciences, University of Aberdeen, Aberdeen, UK

⁶Lancaster Environment Centre, Lancaster University, Lancaster, UK

⁷Centre for Ecology & Hydrology, Lancaster Environment Centre, Lancaster, UK

⁸Imperial College London, Ascot, UK

⁹School of GeoSciences, University of Edinburgh, Edinburgh, UK

Correspondence

David A. Coomes and Tommaso Jucker, Forest Ecology and Conservation group, Department of Plant Sciences, University of Cambridge, Cambridge, UK.
Emails: dac18@cam.ac.uk; tommasojucker@gmail.com

Funding information

Natural Environment Research Council, Grant/Award Number: NE/K016377/1; Sime Darby Foundation

Abstract

Local-scale microclimatic conditions in forest understoreys play a key role in shaping the composition, diversity and function of these ecosystems. Consequently, understanding what drives variation in forest microclimate is critical to forecasting ecosystem responses to global change, particularly in the tropics where many species already operate close to their thermal limits and rapid land-use transformation is profoundly altering local environments. Yet our ability to characterize forest microclimate at ecologically meaningful scales remains limited, as understorey conditions cannot be directly measured from outside the canopy. To address this challenge, we established a network of microclimate sensors across a land-use intensity gradient spanning from old-growth forests to oil-palm plantations in Borneo. We then combined these observations with high-resolution airborne laser scanning data to characterize how topography and canopy structure shape variation in microclimate both locally and across the landscape. In the processes, we generated high-resolution microclimate surfaces spanning over 350 km², which we used to explore the potential impacts of habitat degradation on forest regeneration under both current and future climate scenarios. We found that topography and vegetation structure were strong predictors of local microclimate, with elevation and terrain curvature primarily constraining daily mean temperatures and vapour pressure deficit (VPD), whereas canopy height had a clear dampening effect on microclimate extremes. This buffering effect was particularly pronounced on wind-exposed slopes but tended to saturate once canopy height exceeded 20 m—suggesting that despite intensive logging, secondary forests remain largely thermally buffered. Nonetheless, at a landscape-scale microclimate was highly heterogeneous, with maximum daily temperatures ranging between 24.2 and 37.2°C and VPD spanning two orders of magnitude. Based on this, we estimate that by the end of the century forest regeneration could be hampered in degraded secondary forests that characterize much of Borneo's lowlands if temperatures continue to rise following projected trends.

KEYWORDS

canopy height, digital elevation model, forest degradation and fragmentation, LiDAR, near-surface air temperature, remote sensing, selective logging, vapour pressure deficit

1 | INTRODUCTION

Local-scale microclimatic conditions in forest understoreys shape ecological processes at all levels of organization, from the metabolic and demographic rates of individual organisms to whole-ecosystem nutrient cycling (Chen et al., 1999; Clarke, 2017). Consequently, understanding how the diversity, composition and functioning of forest ecosystems will respond to rapid global change hinges on our ability to quantify microclimate at these ecologically relevant scales (Bramer et al., 2018; De Frenne et al., 2013; Lenoir, Hattab, & Pierre, 2017). Yet doing so remains inherently challenging, as understorey microclimatic conditions cannot be directly measured from outside the canopy. As a result, for most applications we still rely heavily on coarse-resolution interpolated climate surfaces that not only fail to capture climate at scales that are ecologically meaningful (Potter, Arthur Woods, & Pincebourde, 2013), but are also unrepresentative of conditions below the canopy (De Frenne & Verheyen, 2016). New ways of quantifying variation in understorey microclimate and its underlying drivers at both high resolution and across broad spatial scales are therefore urgently needed (Bramer et al., 2018; Frey et al., 2016; Lenoir et al., 2017).

Nowhere is this need to understand local-scale variation in microclimate more pressing than in tropical forest landscapes, where many species already operate close to their thermal limits (Doughty & Goulden, 2008; Tan et al., 2017; Way & Oren, 2010) and where a combination of land-use intensification and climate change are rapidly altering environmental conditions at both regional and local scales (Duveiller, Hooker, & Cescatti, 2018; Hardwick et al., 2015; McAlpine et al., 2018). Two aspects in particular play a key role in constraining microclimate in forests: topography and vegetation structure. Topography shapes microclimate through well-known adiabatic processes associated with elevation, as well as by influencing exposure to wind and solar radiation, both of which are modified by the slope, aspect and curvature of the terrain (Dobrowski, 2011). Additionally, vegetation structural attributes such as the height, density and roughness of the canopy also strongly influence near-surface microclimatic conditions through shading, by altering airflow and by constraining leaf transpiration (Hardwick et al., 2015). Consequently, land-use change has the potential to drastically modify local microclimatic conditions through its effects on vegetation structure and composition. While recent work suggests that selectively logged forests may be thermally buffered (Senior, Hill, Benedick, & Edwards, 2017; Senior, Hill, González del Pliego, Goode, & Edwards, 2017), there is likely a threshold above which canopy loss results in an strong and abrupt shift in microclimate (Hardwick et al., 2015). Similarly, other processes that influence canopy structure and composition—such as natural disturbances and variation in forest composition and dynamics along topo-edaphic gradients (Jucker, Bongalov, & Burslem, 2018; Werner & Homeier, 2015)—can also indirectly contribute to shaping variation in microclimate across tropical forest landscapes.

Yet while the effects of topography and canopy structure on microclimate are for the most part well understood, characterizing

these processes at high resolution and across broad spatial scales remains challenging. In this regard, emerging remote sensing technologies such as airborne laser scanning (ALS, also known as LiDAR) provide a solution for simultaneously capturing the 3D structure of both the forest canopy and the underlying terrain in exquisite detail (Detto, Muller-Landau, Mascaro, & Asner, 2013; Lefsky, Cohen, Parker, & Harding, 2002; Wulder et al., 2012). By coupling ALS data with on-ground networks of microclimate sensors, we are now in a position to robustly assess the relative importance of different topographic and canopy structural features in determining microclimate (Frey et al., 2016; Lenoir et al., 2017). Moreover, these same data can then be used to generate high-resolution microclimatic surfaces for entire landscapes using either empirical or physical-based modelling approaches (Hardwick, 2015; Tymen et al., 2017). This last step is critical if we are to generate realistic predictions of how ecological communities and the processes they underpin are likely to respond to rapid global change (Lenoir et al., 2017).

Here, we combine ALS data with almost one million hourly readings of near-surface air temperature and vapour pressure deficit (VPD) taken across a land-use intensity gradient that spans from old-growth tropical forests to oil-palm plantations in Malaysian Borneo. These data were used to fit empirical models relating variation in microclimate among sites to topographic and canopy structural attributes derived from ALS. We then used these models to generate high-resolution air temperature and VPD surfaces over an area of more than 350 km² to characterize how microclimate varies across human-modified tropical landscapes. From these, we developed a series of scenarios to explore how habitat degradation might impact forest regeneration under present-day and future climate conditions based on our current understanding of how tropical tree seedlings respond to elevated VPD. Finally, we compared our up-scaled microclimate surfaces with coarse-resolution interpolated climate grids routinely used as inputs for ecological models. By doing so, we aimed to determine whether the two differ systematically, and if so whether accounting for the buffering effect of forest canopies on near-surface air temperature can explain these differences.

2 | MATERIALS AND METHODS

2.1 | Study region

The study was conducted in the Malaysian state of Sabah in north-eastern Borneo. Sabah's climate is tropical, with a mean annual temperature of 26.7°C and an annual rainfall of 2,600–3,000 mm (Walsh & Newbery, 1999). The region supports a variety of forests types, including lowland dipterocarp forests that are among the tallest in the tropics. Yet since the 1970 s much of Sabah's forests have been extensively logged and cleared to make way for oil-palm plantations (Gaveau et al., 2016, 2014). To better understand the implications of this land-use transformation for local-scale climatic conditions across the region, here we leverage ALS and microclimate data acquired as part of the Stability of Altered Forest Ecosystems (SAFE) project—one of the world's largest forest fragmentation and degradation

experiments currently underway in Sabah (Ewers et al., 2011). The SAFE project aims to quantify the ecological consequences of forest transformation on a landscape-scale. It spans across a topographically diverse landscape (elevational range: 100–960 m.a.s.l.) made up of forest patches that have been subjected to varying degrees of logging intensity. This includes unlogged old-growth forests, forests that have been selectively logged either once or twice, ones that have been intensively logged over multiple cycles, as well as areas that have been clear-felled and converted to oil-palm plantations (for further details on the logging history of the study site, see Ewers et al., 2011).

2.2 | Microclimate data

Air temperature (T , in °C) and relative humidity (RH, in %) were measured across a network of 113 permanent forest plots established through the SAFE project (each 25×25 m in size). This includes plots in the Kalabakan Forest Reserve and surrounding oil-palm landscape (hereafter collectively referred to as the “SAFE landscape”; $4^{\circ}3'N$, $117^{\circ}2'E$) and in old-growth forests at Maliau Basin Conservation Area ($4^{\circ}5'N$, $116^{\circ}5'E$). Collectively, these plots cover the full land-use intensity gradient captured by the SAFE project—from unlogged old-growth forests to mature oil-palm plantations. In each plot, Hygrochron iButton loggers (Maxim Integrated, USA) suspended at a height of 1.5 m above the ground and shielded from direct solar radiation were used to record hourly T and RH readings (accurate to $\pm 0.5^{\circ}C$ and $\pm 5\%$, respectively). Microclimate data were collected between May 2013 and March 2015, resulting in a total of 953,789 coupled T and RH readings. Due to sensors malfunctioning or being lost in the field, data from four plots were excluded from all further analyses as microclimate readings at these sites spanned less than three months (see Supporting Information Figure S1; In Appendix S1).

Additionally, microclimate data were also acquired in seven Global Ecosystem Monitoring (GEM) 1-ha plots that cover the same logging intensity gradient described above (Riutta et al., 2018). This includes four plots in forests that have been either intensively or selectively logged twice in the SAFE landscape and three old-growth forest plots with no history of logging—one located at Maliau Basin, the other two at Danum Valley Conservation Area ($4^{\circ}6'N$, $117^{\circ}4'E$). Hourly T and RH measurements were recorded using HOBO U23 Pro v2 loggers (Onset Computer Corporation, USA; accuracy: $\pm 0.2^{\circ}C$ and $\pm 5\%$) placed at 1.5 m above the forest floor and shielded from direct sunlight. Data were collected between July 2015 and May 2016, but only measurements from 2015 were used for our analysis ($n = 20,052$), as 2016 was characterized by higher-than-average temperatures that coincided with the strong El Niño event that affected South-East Asia that year (see Appendix S1; Thirumalai, DiNezio, Okumura, & Deser, 2017).

2.2.1 | Microclimate variables

From the hourly temperature records, we calculated the mean annual temperature (T_{mean}) and the mean maximum daily temperature (T_{max}) of

each study plot. T_{mean} and T_{max} directly influence biological activity and habitat suitability across a range of taxonomic groups that are key to shaping the biodiversity and ecosystem functioning of tropical forests, including microbes, fungi, plants, invertebrates and vertebrates (Clarke, 2017). We focus on metrics that integrate temperature conditions across the course of the year as our data show little evidence of seasonal trends in temperature, with differences in temperature between plots far exceeding any systematic variation across seasons (Figure S2). This is in line with previous studies that have shown that with the exception of El Niño years, the climate at our study site is largely aseasonal (Walsh & Newbery, 1999).

In addition to air temperature, we also used the microclimate data to characterize atmospheric water balance by estimating VPD (in hPa). VPD is the difference between the saturation water vapour pressure (e_s) and the actual water vapour pressure (e)—in other words the difference between how much moisture the air can hold before becoming saturated and the amount of moisture actually present in the air. As such, VPD is intimately linked to water transport and transpiration in plants (Anderson, 1936; Motzer, Munz, Kupperts, Schmitt, & Anhof, 2005; Will, Wilson, Zou, & Hennessey, 2013), with high VPD driving reduced growth and survival in both temperate and tropical trees (McDowell et al., 2018; Sanginés de Cárcer et al., 2018). Given that $RH = (e/e_s) \times 100$, VPD can be expressed as $[(100 - RH)/100] \times e_s$, where e_s is derived from T using Bolton's (1980) equation: $e_s = 6.112 \times e^{\frac{17.62 \times T}{T + 243.5}}$. Having estimated VPD for each coupled hourly observation of T and RH, we then calculated annual mean VPD (VPD_{mean}) and mean daily maximum VPD (VPD_{max}) for each study plot.

2.3 | Airborne laser scanning data

ALS data covering the SAFE project were acquired in November 2014 using a Leica ALS50-II LiDAR sensor flown by NERC's Airborne Research Facility. Data acquisition parameters and processing are described in detail in Jucker, Asner, and Dalponte (2018). Briefly, the data were obtained as a discretized point cloud, with up to four returns recorded per pulse and a median density of $15.3 \text{ pulses m}^{-2}$. Points were classified into ground and nonground returns using the LAsTools software (<https://rapidlasso.com/lastools>), and a digital elevation model (DEM) was fit to the ground returns to produce a 1-m resolution raster. The DEM was then subtracted from the elevations of all nonground returns to produce a normalized point cloud, from which a 0.5-m resolution pit-free canopy height model (CHM) was generated following the approach described in Khosravipour, Skidmore, Isenburg, Wang, and Hussin (2014).

All further processing of the ALS data was done using the *raster* package in R (Hijmans, 2016; R Core Development Team, 2016) and custom-written Python code. Specifically, for both the field plots and the SAFE landscape as a whole, we used the DEM, CHM and normalized point clouds to calculate a series of topographic and canopy structural and metrics relevant for characterizing microclimate (described below). For the SAFE plots, metrics were extracted after applying a 12.5-m buffer around each plot, bringing the plot size to 50×50 m. This was done to ensure that canopy conditions around

the perimeter of each plot were captured, as forest clearings (both natural and man-made) can modify understorey microclimatic conditions tens of metres from the forest edge (Camargo & Kapos, 1995; Chen et al., 1999; Ewers & Banks-Leite, 2013). For consistency, we applied this same approach to the GEM plots, extracting ALS metrics from a 50 × 50 m area centred on the location of the microclimate loggers. Similarly, all landscape-scale level metrics were computed at 50-m resolution.

2.3.1 | Topographic metrics

From the DEM, we extracted four topographic metrics known to affect air temperature and humidity through changes in atmospheric pressure or exposure to wind and solar radiation (Dobrowski, 2011): elevation (in m.a.s.l.), terrain slope (in degrees), aspect (in radians) and topographic position index (TPI), which describes the curvature of the terrain and ranges from negative where the terrain is concave (i.e., gulleys) to positive where it is convex (i.e., ridges). As the study site lies near the equator and prevailing winds in the region blow from the east, we expect differences in exposure to wind and solar radiation to be most pronounced between east and west-facing slopes. To capture this, aspect values were sine-transformed so that east-facing slopes are assigned positive values, while leeward slopes facing west are characterized by negative ones. For each plot and landscape grid cell, elevation was calculated by taking the mean value of the DEM within an area of 50 × 50 m. Prior to calculating slope, aspect and TPI, we first spatially resampled the DEM to 10-m resolution, at which point mean values for each metric were extracted at 50 × 50 m. This two-step approach ensured that slope, aspect and TPI estimates were not unduly affected by extreme localized values (Jucker, Bongalov, et al., 2018).

2.3.2 | Canopy structural metrics

From the CHM and the normalized ALS point cloud, we calculated five canopy structural metrics related to canopy height, density, openness and roughness which we hypothesize to influence understorey microclimate as a result of shading and modified air flow. These included maximum canopy height (H_{\max} , in m), mean top-of-canopy height (TCH, in m), gap fraction at 2 m aboveground (in %), standard deviation of TCH (in m) and plant area index (PAI, in $\text{m}^2 \text{m}^{-2}$), a measure of the total plant area (leaves and woody tissues) per unit ground surface area. PAI is an integrated measure of canopy density which we estimated empirically from the ALS point cloud using the MacArthur-Horn approximation following the approach of Stark et al. (2012).

While these metrics aim to capture complementary aspects of canopy structure, they are nonetheless inherently related to one another (Appendix S2). To avoid issues with collinearity in our models, a preliminary analysis was conducted to ascertain which canopy metric would be best suited for modelling microclimate. This revealed two primary axes of variation, one related to canopy height, the other to canopy density (Appendix S2). Based on this, we chose to focus our analyses of H_{\max} and PAI as predictors of understorey

microclimate. To completely remove collinearity between model predictors, we then fit a regression linking variation in PAI to H_{\max} (both log-transformed) and took the residual variation in PAI from this model ($\text{PAI}_{\text{resid}}$) as a predictor for all further analyses presented here. High values of $\text{PAI}_{\text{resid}}$ indicate canopies that are denser than expected based on their height, while low values correspond to sparser and more open canopies.

2.4 | Plot-level microclimate modelling

We used a structural equation modelling (SEM) framework to characterize how land-use intensity, canopy structure and topography interact to shape local-scale variation in microclimate. In a first step, data from the 116 plots with microclimate records were used to fit multiple regression models relating variation in T_{mean} , T_{\max} , VPD_{mean} and VPD_{\max} to the topographic and canopy structural metrics described above. In the case of VPD_{mean} and VPD_{\max} , the models also explicitly accounted for the effects of air temperature on VPD, as the two are intrinsically related (i.e., for a given RH, increasing T drives an increase in VPD). Additionally, we tested for specific interaction terms between canopy structural metrics and topographic ones—namely H_{\max} , aspect and TPI—as we expect canopy effects on microclimate to be most pronounced on exposed, west-facing slopes and on hilltops. Based on a visual inspection of the data, T_{mean} , T_{\max} and H_{\max} were log-transformed prior to model fitting to better capture the relationship between air temperature and canopy height and normalize the residuals of the model.

In addition to modelling the direct effects of topography and canopy structure on microclimate, we also fit regression models relating plot-level variation in H_{\max} and $\text{PAI}_{\text{resid}}$ to topographic metrics, allowing us to characterize the indirect effects of topography on air temperature and VPD mediated through changes in canopy structure (Jucker, Bongalov, et al., 2018; Werner & Homeier, 2015). This analysis was also repeated across the entire SAFE landscape, allowing us to leverage the full coverage of the ALS data (approximately 363 km^2). Lastly, we indirectly linked variation in microclimate to logging history and land-use intensity by characterizing changes in canopy structural metrics along the land-use intensity gradient captured by the SAFE project.

In a second step, we then brought together the individual regression models using a piecewise SEM framework (also known as confirmatory path analysis), as implemented in the *piecewiseSEM* package in R (Lefcheck, 2016). This allowed us to visually and quantitatively assess the direct and indirect impacts of topography, canopy structure and land-use intensity on microclimatic variation. To obtain standardized path coefficients—the magnitude of which can be directly compared within and between submodels—all data were scaled prior to model fitting to have a mean of 0 and standard deviation of 1. Lastly, in order to determine whether variation in T_{mean} , T_{\max} , VPD_{mean} and VPD_{\max} was most strongly associated with topography or canopy structure, we used variance partitioning to assign R^2 values to each model predictor using the recommended “averaging over orderings” approach proposed by Lindeman, Merenda, and Gold (1980) as implemented in the R package *relaimpo* (Grömping, 2006).

2.5 | Landscape-scale variation in microclimate and its implications for forest regeneration

The best-fit regression models for T_{mean} , T_{max} , VPD_{mean} and VPD_{max} were used to map each microclimate variable at 50-m resolution across the SAFE landscape ($n = 145,214$ grid cells, equivalent to approximately 363 km^2) using DEM, CHM and point cloud-derived metrics as inputs.

To showcase how high-resolution microclimate data can be used to better understand and forecast responses of tropical forests to global change, we used our up-scaled estimates of VPD_{max} to identify areas within the SAFE landscape where conditions might be suboptimal for forest regeneration under current and future climate conditions. Specifically, we first quantified what proportion of the SAFE landscape currently experiences mean daily maximum VPD values that exceed 12 hPa, threshold above which VPD has been shown to impede transpiration in montane Neotropical trees (Motzer et al., 2005). We then repeated this after accounting for changes in VPD_{max} that are expected to occur by 2080 as a result of increases in T_{max} predicted by the HadGEM2-AO general circulation model for two Representative concentration pathways (RCP) presented in the IPCC's Fifth Assessment Report (IPCC, 2014). The first is an emission mitigation scenario (RCP4.5), under which T_{max} is expected to increase by 1.9°C across the SAFE landscape by 2061–80. The second is a business-as-usual scenario (RCP8.5) which predicts T_{max} will increase by 2.8°C at SAFE by 2061–80 (estimates based on future climate projections obtained at 30-arc second resolution from: <https://www.worldclim.org/CMIP5v1>).

Note that this analysis makes a number of important assumptions and is only intended to provide an approximate estimate of how climate change could impact the regeneration of tropical forests in human-modified landscapes. For instance, it assumes no further land-use intensification in the study area, nor does it account for changes in rainfall regimes. This is despite the fact that there is already evidence of declines in precipitation in regions affected by high deforestation rates in Borneo (McAlpine et al., 2018). Additionally, there may well be differences in the ecophysiological responses of Bornean tree species to VPD compared to those of the Neotropical montane species studied in Motzer et al. (2005), although we note that both systems are characterized by relatively aseasonal climates and that in selecting a VPD threshold of 12 hPa we adopted the upper limit identified in the above-mentioned study. Nonetheless, to assess how sensitive our estimates are to the choice of VPD threshold, we repeated the analysis assuming a VPD_{max} of 15 hPa as a limit to transpiration, which is in line with recent estimates for temperate tree species in Europe (Sanginés de Cárcer et al., 2018).

2.6 | Comparing up-scaled microclimate surfaces with coarse-resolution gridded climate data

In addition to using the up-scaled microclimate estimates to identify areas where evaporative demands could impede forest regeneration, we also compared them to coarser-resolution gridded climate data from the WorldClim2 database that underpin a wide range of ecological

modelling applications (Fick & Hijmans, 2017). WorldClim2 climate grids are generated by interpolating observations from weather stations typically located in open environments and have a spatial resolution of 30-arc seconds (approximately 1 km). Here, we focus on two WorldClim2 variables—mean annual temperature and mean monthly maximum temperature—which we compared to our up-scaled estimates of T_{mean} and T_{max} . To enable comparisons between the two, we extracted mean and maximum air temperature values from the WorldClim2 layers for each 50-m grid cell covering the SAFE landscape. This allowed us to determine whether up-scaled microclimate estimates differ systematically from WorldClim2 gridded temperature surfaces (Faye, Herrera, Bellomo, & Dangles, 2014), with potentially important consequences for how we currently forecast the impacts of climate change across ecological scales. Moreover, it allowed us to explore whether accounting for the buffering effect of forest canopies on near-surface air temperature—which is not captured by WorldClim2 (De Frenne & Verheyen, 2016)—helps explain any systematic differences we see between micro- and macroclimate data.

3 | RESULTS

3.1 | Topographic and canopy structural effects on microclimate

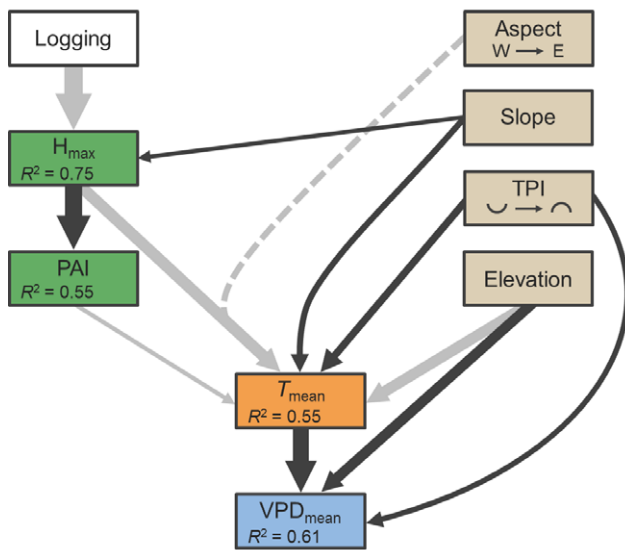
3.1.1 | Mean and maximum air temperature

Both topography and canopy structure helped explain differences in air temperature among forest plots (Figure 1) and together accounted for 55% of the variation in T_{mean} and 57% of that in T_{max} (see Appendix S3 for full summaries of all regression models). Generally, both T_{mean} and T_{max} were lower under tall, dense forests canopies (i.e., ones with high H_{max} and $\text{PAI}_{\text{resid}}$), at higher elevations within the landscape and in gulleys, where TPI values are negative (Figure 2). T_{mean} was influenced more strongly by topography than canopy structure (Figure 1b), and all else being equal decreased by 0.4°C for every 100 m of elevation gain (Figure 2b). By contrast, variation in T_{max} was predominately controlled by canopy structure, with H_{max} alone explaining 36% of the variance in T_{max} (Figure 1d). This effect of canopy height on air temperature was markedly nonlinear and tended to plateau past a certain H_{max} for both T_{mean} and T_{max} . Specifically, after controlling for the effects of topography, we estimate that 20-m tall forests have a T_{mean} and T_{max} that are 1.8°C and 5.9°C cooler, respectively, compared to areas with no vegetation cover above 1 m (Figure 2a,d). However, extending canopy height by a further 20 m only led to an additional decrease in T_{mean} of 0.4°C and in T_{max} of 1.2°C . As a result, we found that despite intensively logged forest plots having canopies that are, on average, only half as tall as those of old-growth ones (mean $H_{\text{max}} = 32.2 \text{ m}$ compared to 64.0 m ; Figure 3), the two differed in T_{mean} and T_{max} by just 0.4°C and 1.2°C , respectively.

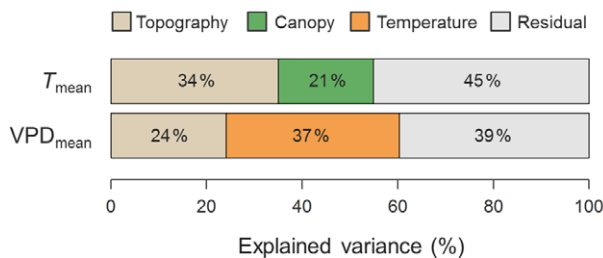
The effects of topography and canopy structure on air temperature were more than just additive. Firstly, in both the T_{mean} and T_{max} models we found clear evidence of an interaction between aspect and H_{max} (Figure 1), whereby the influence of canopy height on air

Mean temperature and VPD

(a)

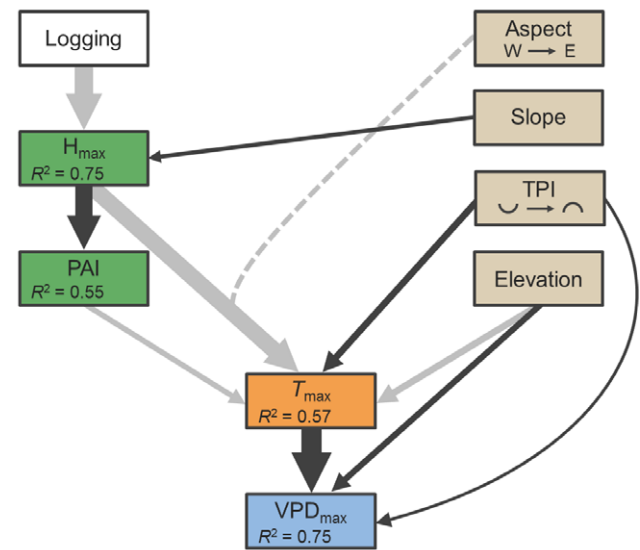


(b)



Maximum temperature and VPD

(c)



(d)

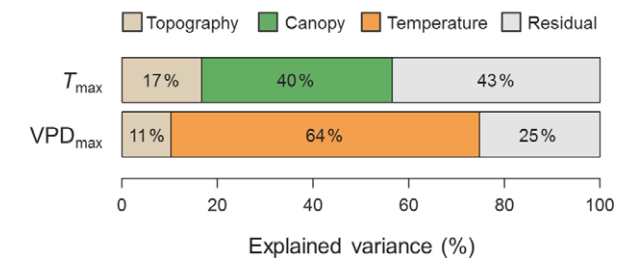
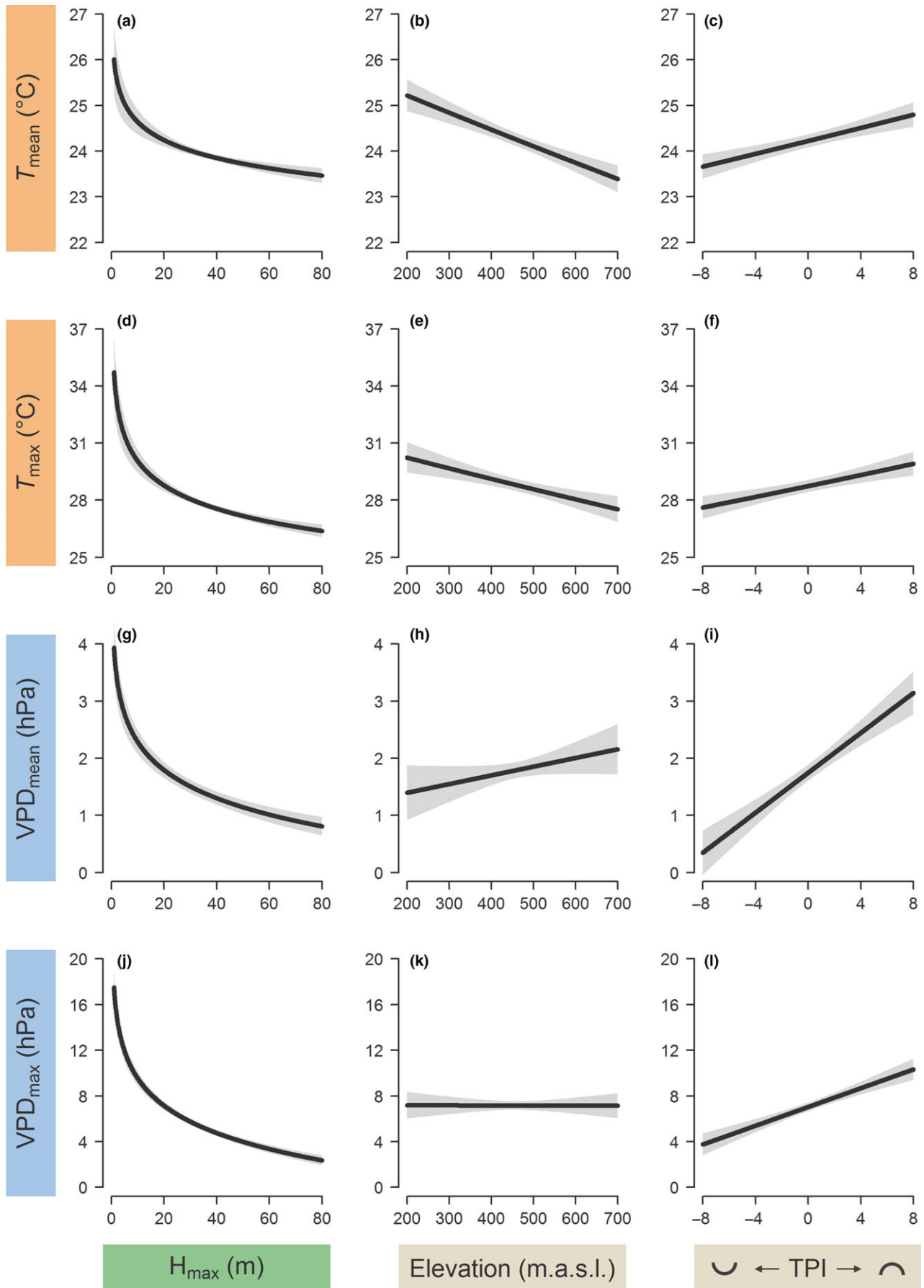


FIGURE 1 Piecewise structural equation models relating variation in (a) annual mean temperature (T_{mean}) and vapour pressure deficit (VPD_{mean}) and (b) mean maximum daily temperature (T_{max}) and vapour pressure deficit (VPD_{max}) to canopy structural and topographic metrics. The models also capture the effects of logging pressure and land-use intensity on maximum canopy height (H_{max}), as well as the covariation between H_{max} and plant area index (PAI)—which was explicitly accounted for by taking the residuals of a regression relating PAI to H_{max} as a predictor of temperature and VPD in the models. Dark grey arrows denote positive relationships, while light ones correspond to negative associations. The width of the arrows reflects the strength of the pathway and is proportional to the standardized path coefficient (reported in Appendix S3). A dashed arrow was used to represent the interaction effect between aspect and H_{max} . Only pathways that were significant to $p \leq 0.05$ are shown. R^2 values are reported for each endogenous variable. Additionally, panels (b) and (d) provide a breakdown of how much of the variance in T_{mean} , VPD_{mean} , T_{max} and VPD_{max} was explained by topographic metrics, canopy structural metrics and (in the case of VPD) by temperature [Colour figure can be viewed at wileyonlinelibrary.com]

temperature was markedly stronger on wind-exposed, east-facing slopes. Specifically, we estimate that increasing H_{max} from 1 to 20 m on east-facing slopes resulted in a decrease in T_{mean} of 3.1°C and in T_{max} of 8.7°C. By contrast, this same increase in H_{max} on leeward, west-facing slopes only drove a decrease in T_{mean} of 0.6°C and in

T_{max} of 3.6°C. Additionally, we also found that topography can influence air temperature indirectly through its effects on canopy structure. Forest plots on steeper slopes were characterized by taller canopies (Figure 1), a pattern that also emerged at landscape-scale (see Appendix S4 for model outputs). Across the broader landscape,

FIGURE 2 Modelled relationships between microclimate variables and forest structural and topographic attributes, including maximum canopy height (H_{max}), elevation and topographic position index (TPI). Response curves for mean annual temperature (T_{mean}), mean maximum daily temperature (T_{max}), mean annual vapour pressure deficit (VPD_{mean}) and mean maximum daily vapour pressure deficit (VPD_{max}) correspond to predicted values ($\pm 95\%$ confidence intervals) obtained from the regression models which underpin the structural equation models depicted in Figure 1. For T_{mean} and T_{max} , fitted values were obtained by setting all model predictors (except those presented on the x-axis) to their global mean values. For VPD_{mean} and VPD_{max} , predicted values account for both the direct effects of the canopy structural and topographic variables on VPD (while keeping all other model predictors constant at their mean value) as well as those mediated through changes in air temperature driven by H_{max} , elevation and TPI [Colour figure can be viewed at wileyonlinelibrary.com]



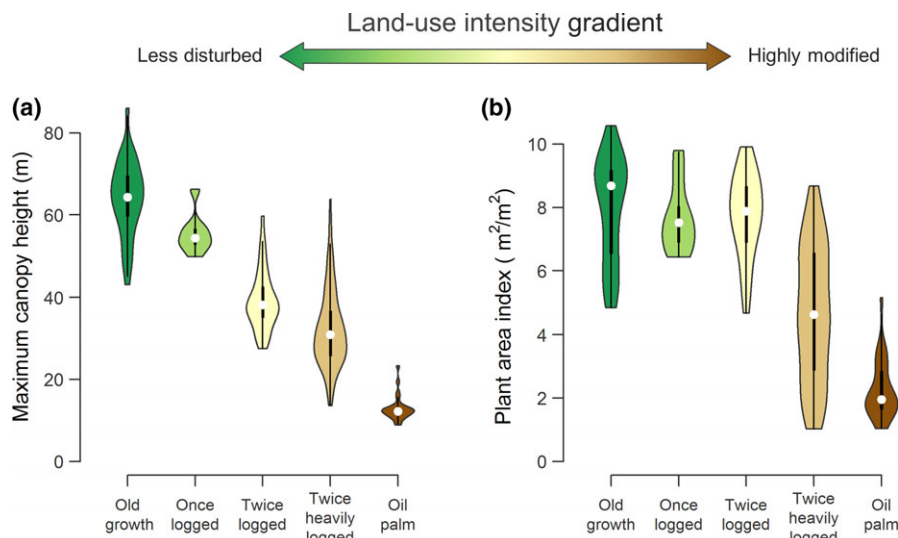


FIGURE 3 Variation in (a) maximum canopy height and (b) plant area index along in relation to land-use intensity and historical logging pressure across the Stability of Altered Forest Ecosystems (SAFE) and Global Ecosystem Monitoring (GEM) plots [Colour figure can be viewed at wileyonlinelibrary.com]

ALS data also suggest that forests in gulleys (defined as areas with $\text{TPI} \leq -6$) attained maximum heights that were 10.7 m greater, on average, than those on hilltops and ridges ($\text{TPI} \geq 6$), and that forests on east-facing slopes were up to 3.6 m shorter than those on the more protected west-facing ones (Appendix S4).

3.1.2 | Mean and maximum vapour pressure deficit

The effects of topography and canopy structure on VPD were predominantly mediated through changes in local air temperature, rather than a direct influence on VPD (Figure 1). Regression models explained 61% of the variance in VPD_{mean} and 75% of that in VPD_{max} , with most of this attributed to changes in T_{mean} and T_{max} . Topographic features did, however, explain 24% of the variance in VPD_{mean} , which—for a given temperature—tended to increase with both elevation and TPI. The same pattern, although less pronounced, was also found for VPD_{max} .

When accounting for the indirect effects of topography and canopy structure on air temperature, both VPD_{mean} and VPD_{max} were found to decrease rapidly with increasing canopy height and density before tending to plateau in plots where H_{max} exceeded 40 m (Figure 2g,j). Similarly, as TPI was positively correlated with both T and VPD (Figure 1), terrain curvature had a compound effect on VPD such that—all else being equal—forests on ridges and hilltops ($\text{TPI} \geq 6$) were estimated to have a VPD_{mean} that was four times that of forests in gulleys ($\text{TPI} \leq -6$; 0.7 hPa compared to 2.8 hPa; Figure 2i), and a VPD_{max} that was more than twice as high (4.6 hPa compared to 9.5 hPa; Figure 2l). By contrast, because VPD (for a given air temperature) tended to increase with elevation while T decreased (Figure 1), both VPD_{mean} and VPD_{max} remained fairly constant across the elevational gradient present at SAFE (Figure 2h,k).

3.2 | Landscape-scale variation in microclimate and its implications for forest regeneration

Up-scaled microclimate estimates varied considerably across the SAFE landscape (Figure 4), with T_{mean} ranging between 22.0 and

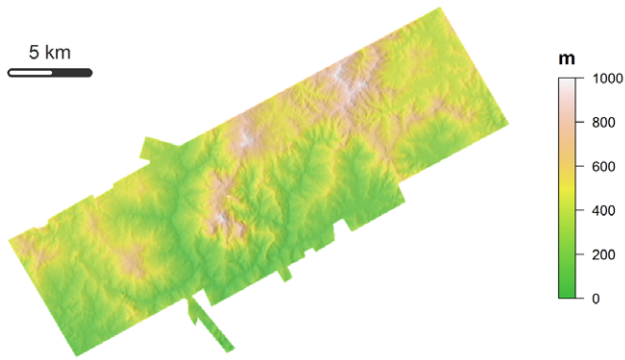
27.7°C (mean = 24.5°C), T_{max} between 24.2 and 37.2°C (mean = 29.5°C), VPD_{mean} between 0 and 4.5 hPa (mean = 1.8 hPa) and VPD_{max} between 0 and 18.5 hPa (mean = 7.8 hPa).

Under present-day conditions, our models predict that 14.5% of the area covered by our ALS campaign currently experiences mean maximum daily VPD values in excess of 12 hPa (Figure 5a,c), threshold above which evaporative demands are expected to impede growth and results in increased risk of mortality for tropical tree seedlings. Under the RCP4.5 emission scenario—which predicts an increase in T_{max} of 1.9°C by 2080—we forecast that the proportion of the SAFE landscape categorized as suboptimal for forest regeneration would more than double to 32.6% even if no further forest clearing were to take place and rainfall regimes were to remain unchanged (Figure 5a). This increase would be even more substantial under the RCP8.5 business-as-usual scenario, reaching 49.1% of the SAFE landscape (Figure 5c). Adopting a more conservative VPD_{max} threshold to leaf transpiration and photosynthesis of 15 hPa, our estimates of the proportion of the study area where conditions are currently suboptimal for seedling establishment and growth were revised down to 5.3% (Figure 5b,d). Nonetheless, even in this scenario a rise in T_{max} of 1.9°C and 2.8°C by 2080 (RCP4.5 and RCP8.5, respectively) would still result in a more than threefold increase in the area where forest regeneration is potentially impacted by high VPD_{max} (15.3% and 22.4% of pixels, respectively; Figure 5b,d).

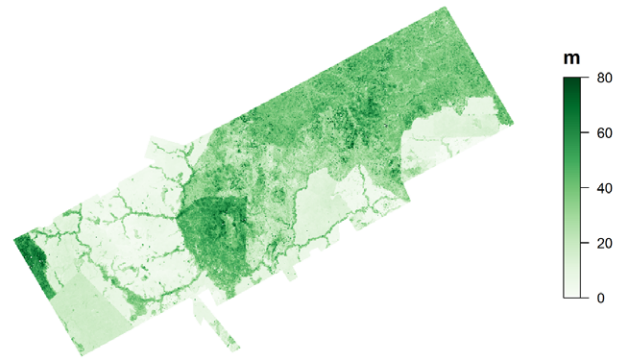
3.3 | Systematic differences between up-scaled microclimate surfaces and WorldClim2 grids

When compared to coarser-resolution gridded climate surfaces, we found that on average air temperature estimates from the WorldClim2 database tended to systematically overestimate T_{mean} by 1.4°C and T_{max} by 1.9°C across the landscape (Figure 6a,c). The discrepancy between mean annual temperatures captured by WorldClim2 grids and those captured by our analysis was explained, in large part, by the cooling effect of the canopy. Areas of the

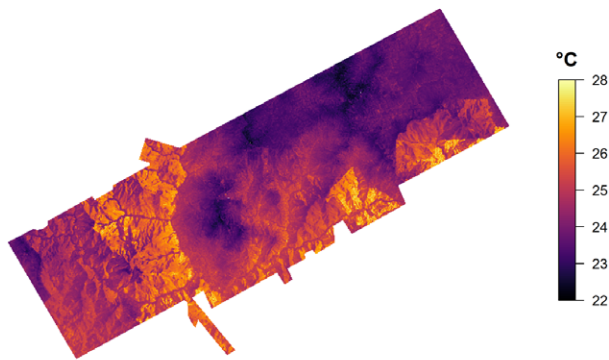
(a) Elevation



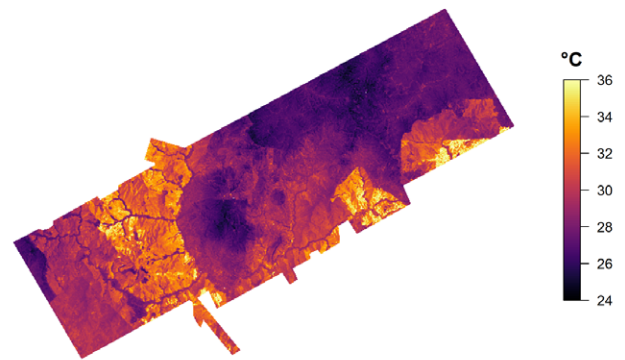
(b) Maximum canopy height



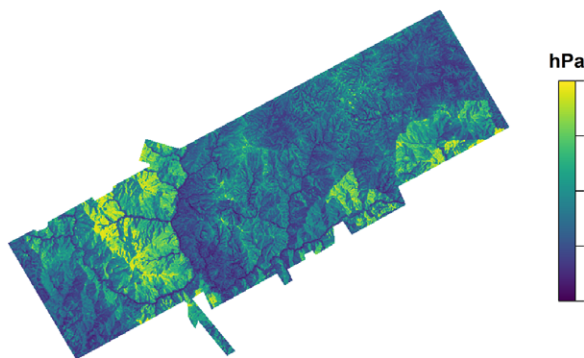
(c) Mean temperature



(d) Maximum temperature



(e) Mean vapour pressure deficit



(f) Maximum vapour pressure deficit

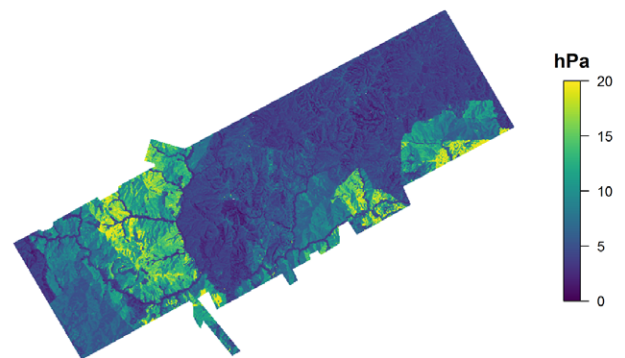


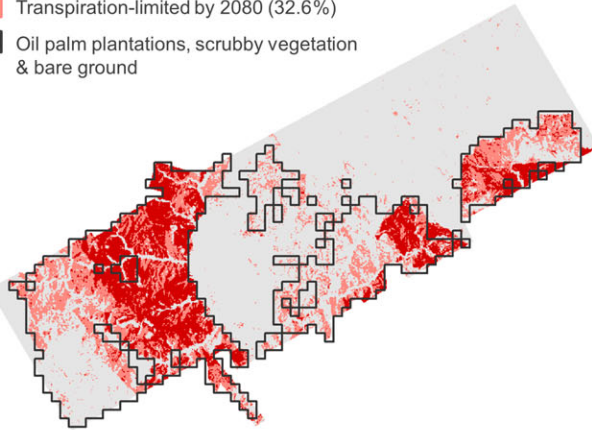
FIGURE 4 Variation in (a) elevation, (b) maximum canopy height, (c) mean annual temperature, (d) mean maximum daily temperature, (e) mean annual vapour pressure deficit and (f) mean maximum daily vapour pressure deficit across the Stability of Altered Forest Ecosystems (SAFE) landscape at 50×50 m resolution. Panels (c–f) correspond to predicted values obtained from the regression models described in the main text and illustrated in Figure 1 [Colour figure can be viewed at wileyonlinelibrary.com]

landscape characterized by little or no vegetation cover ($H_{\max} \leq 2$ m) showed good agreement between microclimate estimates and WorldClim2 grids (mean difference $< 0.1^\circ\text{C}$; standard deviation = 0.9°C ; Figure 6b). Instead, for pixels where $H_{\max} \geq 20$ m WorldClim2 estimates of T_{mean} were 1.7°C warmer than our microclimate ones

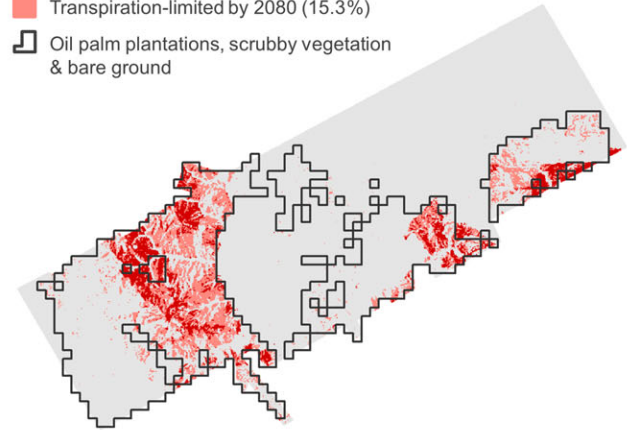
(standard deviation = 0.3°C). Much the same pattern emerged for T_{\max} (Figure 6d). However, in this case even after accounting for canopy effects we still found a clear systematic difference between microclimate estimates and WorldClim2 grids. Specifically, for areas where $H_{\max} \leq 2$ m WorldClim2 estimates were 4.9°C cooler

(a) RCP4.5 scenario (+1.9°C by 2080) assuming 12 hPa threshold to transpiration

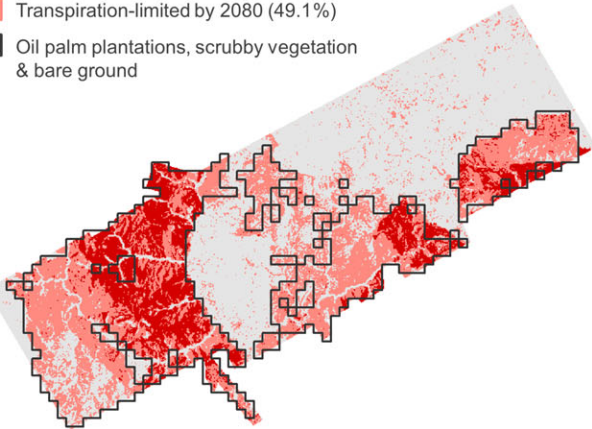
■ Currently limiting for transpiration (14.5%)
 ■ Transpiration-limited by 2080 (32.6%)
 □ Oil palm plantations, scrubby vegetation & bare ground

**(b)** RCP4.5 scenario (+1.9°C by 2080) assuming 15 hPa threshold to transpiration

■ Currently limiting for transpiration (5.3%)
 ■ Transpiration-limited by 2080 (15.3%)
 □ Oil palm plantations, scrubby vegetation & bare ground

**(c)** RCP8.5 scenario (+2.8°C by 2080) assuming 12 hPa threshold to transpiration

■ Currently limiting for transpiration (14.5%)
 ■ Transpiration-limited by 2080 (49.1%)
 □ Oil palm plantations, scrubby vegetation & bare ground

**(d)** RCP8.5 scenario (+2.8°C by 2080) assuming 15 hPa threshold to transpiration

■ Currently limiting for transpiration (5.3%)
 ■ Transpiration-limited by 2080 (22.4%)
 □ Oil palm plantations, scrubby vegetation & bare ground

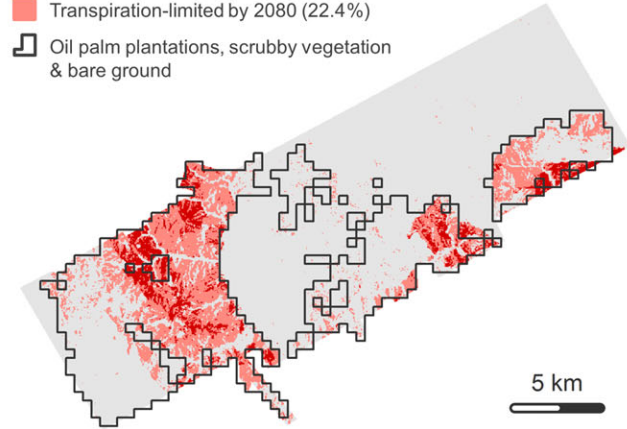


FIGURE 5 Areas of the SAFE landscape where mean maximum daily vapour pressure deficit (VPD_{max}) is predicted to exceed hypothesized transpiration thresholds (12 and 15 hPa) for tree seedlings under current (dark red) and future climate conditions (light red). Results for two different IPCC representative concentration pathways (RCP) are shown: the RCP4.5 emission mitigation scenario (a and b) and the RCP8.5 business-as-usual scenario (c and d). The percentage of 50×50 m pixels exceeding VPD_{max} thresholds is given in brackets for each scenario. The black contour lines mark the current extent of oil-palm plantations within the SAFE landscape, as well as areas dominated by short scrubby vegetation that develops in the aftermath of logging and of bare ground [Colour figure can be viewed at wileyonlinelibrary.com]

compared to our microclimate ones (standard deviation = 1.2°C), whereas for pixels with $H_{max} \geq 20$ m WorldClim2 grids tended to overestimate T_{max} by 2.3°C (standard deviation = 0.8°C).

4 | DISCUSSION

Canopy structure and topography emerged as strong, interactive drivers of fine-scale variation in understorey microclimatic conditions across a land-use intensity gradient that increasingly typifies much of Borneo's lowland tropical landscapes (Bryan et al., 2013; Gaveau

et al., 2014, 2016). Given the importance of local-scale microclimatic conditions in shaping ecosystem responses to global environmental change (De Frenne et al., 2013)—and the fact that currently available climate data tend to be unrepresentative of understorey conditions (De Frenne & Verheyen, 2016; Faye et al., 2014)—our results highlight the potential of remote sensing technologies such as ALS for characterizing microclimate at ecologically relevant scales (Bramer et al., 2018; Frey et al., 2016; Lenoir et al., 2017). Here, we start by taking a closer look at the role of vegetation structure and topography in shaping understorey microclimate in human-modified tropical

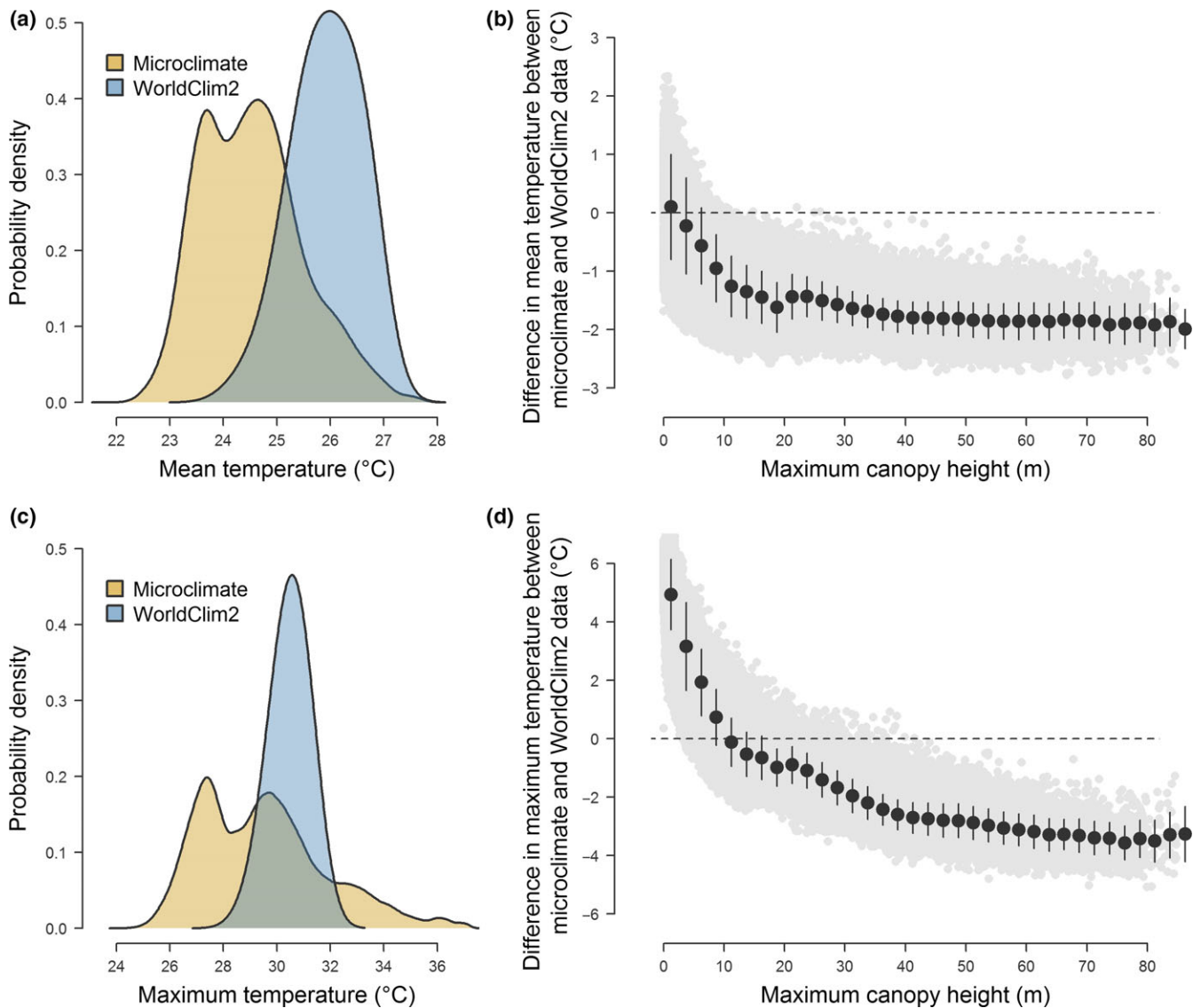


FIGURE 6 Systematic differences between ALS-derived understorey microclimatic conditions and WorldClim2 gridded climate surfaces. Panel (a) shows the probability density distribution of mean annual temperature values predicted from ALS-derived canopy structural and topographic metrics across the Stability of Altered Forest Ecosystems (SAFE) landscape (as mapped in Figure 4c) and those obtained from the WorldClim2 database for the same area. Panel (b) illustrates how—for a given point within the SAFE landscape—the difference between these two temperature surfaces changes according to the maximum canopy height of that pixel. Large black circles correspond to mean difference values (± 1 standard deviation) calculated at 2 m height intervals. Panels (c and d) show these same patterns for maximum temperature [Colour figure can be viewed at wileyonlinelibrary.com]

forests. We focus in particular on some of the more subtle—yet strong—indirect and interactive effects of canopy height, terrain curvature and aspect that traditional field-based approaches would have likely overlooked. We then take a closer look at how ALS-derived microclimate surfaces can refine our understanding of the ecological impacts of global change, using our analysis exploring the potential impacts of climate warming on forest regeneration across the SAFE landscape as a case study. Finally, we end by discussing how the next generation of satellite-based remote sensing platforms could be used to build on our efforts to map the near-surface air temperature and VPD of tropical landscapes, potentially opening the door to microclimate monitoring on a global scale.

4.1 | Canopy structure and topography as drivers of understorey microclimate

Canopy height—which correlated strongly with canopy density and roughness—emerged as an overarching driver of near-surface air temperature and moisture content, with taller canopies being associated with lower mean and maximum temperatures as well VPD (Figures 1 and 2). Vegetation structure influenced air temperature and VPD primarily by dampening maximum daily values rather than strongly shifting their means (Figure 1; Frey et al., 2016). This buffering effect was markedly nonlinear, being strongest in forest patches where the canopy was less than 20 m tall before progressively

saturating thereafter (Figure 2). As a result, we found that even though logging had a profound impact on the height and density of forest canopies (Figure 3; Hardwick et al., 2015; Pfeifer et al., 2016), only under intense logging pressure or following the conversion of forests to oil-palm plantations was microclimate strongly affected. This is broadly consistent with recent work showing that logged forests in the tropics tend to be largely thermally buffered and do not differ substantially in their microclimate to old-growth stands (Senior, Hill, Benedick, et al., 2017; Senior, Hill, González del Pliego, et al., 2017). Yet while previous studies have for the most part been limited to making dichotomous comparisons between logged and unlogged forests, using high-precision ALS data acquired across a landscape where land-use intensity was manipulated experimentally we were able to characterize the effects of forest degradation on microclimate in terms of quantitative changes in forest structure. In doing so, our results underscore the importance of logged and secondary tropical forests not only for their biodiversity (Chazdon et al., 2009; Deere et al., 2018) and carbon storage potential (Martin, Newton, & Bullock, 2013; Poorter et al., 2016; Riutta et al., 2018), but also in terms of their ability to maintain environmental conditions conducive to forest regeneration and nutrient cycling (Both, Elias, Kritzer, Ostle, & Johnson, 2017; Ewers et al., 2015).

By contrast, topography was most important for driving variation in mean annual temperature and VPD across the landscape (Figure 1). In large part, this variation was associated with the elevational gradient that characterizes the SAFE landscape (Figure 2b). Specifically, mean annual temperature was found to decrease by an average of 0.4°C for every 100 m of elevation gain, which is consistent with the adiabatic lapse rate of a warm, fully saturated air parcel (Minder, Mote, & Lundquist, 2010). In addition to elevation, topographic features associated with the slope, curvature and aspect of the terrain—which together influence exposure to wind and solar radiation (Dobrowski, 2011)—were also important in shaping fine-scale variation in microclimate among forest stands. In particular, terrain curvature (as captured by TPI) strongly influenced annual mean VPD (Figure 2i). This occurred as a result of both an indirect effect of TPI on air temperature, whereby ridges were found to be around 0.8°C warmer than gulleys (all else being equal), as well as a direct positive association between terrain concavity and relative humidity. The fact that microclimate can vary so substantially in relation to small-scale terrain features such as those captured here highlights just how important topography can be to shaping the structure, composition and function of tropical forests (Jucker, Bongalov, et al., 2018; Werner & Homeier, 2015).

While the effects of topography on microclimate are for the most part well understood (even if often hard to quantify), what remains much less clear is the extent to which topography and vegetation structure can work together to shape forest microclimate (Frey et al., 2016). In this respect, our results point to a number of subtle, yet strong, interactive and indirect effects linking these two drivers of microclimatic variation. On the one hand, we found clear evidence of an interaction between aspect and canopy height, whereby the buffering effect of canopy structure on near-surface air

temperature was much more pronounced on east-facing slopes. This is consistent with the fact that prevailing winds in the region blow from the east, making the sheltering effect of the canopy more pronounced on these slopes (Hardwick et al., 2015). It may also reflect the fact that in tropical regions clouds tend to build-up during the course of the day, meaning that on average direct solar radiation will be lower on west-facing slopes that are exposed to the sun in the afternoon (Smith, 1977). Consequently, on west-facing slopes forest canopies may play less of a role in intercepting incoming solar radiation before it reaches the forest floor compared to east-facing slopes that are exposed to the morning sun.

In addition to these interactive effects between aspect and canopy height, we also found clear evidence that topography can influence understorey microclimate indirectly by driving fine-scale variation in forest structure within tropical landscapes. Previous work has highlighted the importance of topography in shaping the composition and structure of forest canopies (Jucker, Bongalov, et al., 2018; Swetnam, Brooks, Barnard, Harpold, & Gallo, 2017; Werner & Homeier, 2015), but to our knowledge, the implications of this for understorey microclimate have been largely overlooked. We found that across the SAFE landscape canopy height varied substantially in relation to terrain elevation, slope aspect and curvature (see Appendix S4). While positive associations between canopy height, elevation and terrain slope are likely to primarily reflect logging restrictions on steep slopes (as well as potentially resulting from the tendency of ALS to slight overestimate canopy height on steep ground; Alexander, Korstjens, & Hill, 2018), those between canopy height and topographic position suggest strong underlying ecological gradients. Most notably, we found that forests in gulleys and on leeward slopes sheltered from the wind were substantially taller than those on exposed ridges (also see King, Davies, Tan, & Nur Supardi, 2009; Coomes, Šafka, Shepherd, Dalponte, & Holdaway, 2018), thereby further strengthening underlying microclimatic gradients driven directly by topography.

4.2 | Landscape-scale modelling of microclimate to guide forest conservation

Previous field-based studies have highlighted the extent to which the microclimate of tropical forests can vary as a result of both natural heterogeneity in canopy structure and in response to logging or habitat fragmentation (Ewers & Banks-Leite, 2013; Hardwick et al., 2015; Scheffers et al., 2017; Senior, Hill, Benedick, et al., 2017; Senior, Hill, González del Pliego, et al., 2017). Yet field data alone can only take us so far when the aim is to assess habitat suitability and model ecosystem functioning at scales relevant for management and conservation (Bramer et al., 2018). By combining a network of microclimate sensors with ALS data, we were able to not only identify the key drivers of microclimatic variation within a tropical forest, but also use this information to up-scale air temperature and VPD estimates across the entire landscape at high resolution (Figure 4). Fine-scale microclimate surfaces such as these are critical to forecasting the potential biodiversity impacts of land-use intensification

and regional climate change in human-modified tropical landscapes, particularly for thermally sensitive species characterized by limited dispersal ability (Ehrmann et al., 2017; García-Robledo, Kuprewicz, Staines, Erwin, & Kress, 2016; Kaspari, Clay, Lucas, Yanoviak, & Kay, 2015; Sunday, Bates, & Dulvy, 2011). Moreover, they provide an opportunity to substantially refine models of key ecosystem processes such as soil respiration that currently represent major uncertainties in our understanding of global terrestrial carbon budgets (Bradford et al., 2016; Carey et al., 2016; Jones, Cox, & Huntingford, 2003).

To illustrate the kind of landscape-level inferences made possible by access to high-resolution microclimate surfaces such as those developed here, we explored how land-use intensification might impact forest regeneration under present and future climate scenarios as a result of changes in VPD—which constrains transpiration in plants and is a strong predictor of growth and mortality in tropical trees (McDowell et al., 2018; Motzer et al., 2005; Will et al., 2013). In this respect, our results suggest that under current conditions between 5% and 15% of the SAFE landscape exceeds a VPD threshold above which the survival and growth of tropical tree seedlings could be decreased, leading to suboptimal conditions for forest regeneration (Figure 5). Yet at present, areas classified as suboptimal are almost exclusively located within oil-palm plantations, making the point about potential for forest regeneration rather moot. This outlook changes when we forecast increases in VPD that would result from a rise in regional temperatures by the end of the century, particularly if we assume a threshold to transpiration of 12 hPa (Figure 5a,c). Under these scenarios not only would the proportion of the landscape deemed as suboptimal for seedling growth and survival more than double, but VPD thresholds to transpiration would also be exceeded in parts of the landscape characterized by early-successional, degraded secondary forests (Figure 5c). The microclimate impacts on the successional trajectories of these degraded forest patches would likely be further compounded by soil runoff and nutrient leaching associated with intensive logging activities (Labrière, Locatelli, Laumonier, Freycon, & Bernoux, 2015; Sidle et al., 2006), as well as the progressive loss of a seed bank (Holl, 1999). Consequently, highly disturbed tropical landscapes could become harder to rehabilitate in the future, having to increasingly resort to costly reforestation initiatives rather than relying on natural regeneration (Graham, Laurance, Grech, McGregor, & Venter, 2016). This is particularly true of Sabah where 32% of the land is covered by highly degraded secondary forests (Bryan et al., 2013).

The approach we take to forecasting habitat suitability for tropical seedlings does have a number of clear limitations. For instance, our scenarios are all based on VPD thresholds to transpiration taken from the literature rather than ones measured in situ, on top of which we only account for increases in temperature without factoring in further changes in land-use or rainfall regimes. Moreover, our scenarios overlook the fact that forest degradation would also change light regimes on the forest floor, which would have important implications for seedling establishment and growth. Nonetheless, it highlights why efforts to develop high-resolution, ecologically

meaningful environmental data layers are critical if we are to improve our ability to forecast how tropical forests will respond under growing pressure from logging, habitat fragmentation and climate change. In this regard, we see the current and future scenarios developed here as hypotheses to be tested and refined in the field.

4.3 | Leveraging emerging remote sensing technologies to track microclimate on a global scale

When comparing near-surface air temperature estimates up-scaled using the ALS data to ones obtained through WorldClim2, we found that the latter not only substantially underestimates the degree to which microclimate varies within landscapes (Figure 6a,c), but also departs systematically from understorey microclimate observations (Faye et al., 2014). When averaged across the entire study area, mean annual temperatures obtained from the WorldClim2 database overestimated locally derived values by 1.4°C, which is similar in magnitude to projected warming trends for the region by the end of the century under a conservative emission scenario (Scriven, Hodgson, McClean, & Hill, 2015). In large part, these differences between microclimate estimates and WorldClim2 grids could be explained by the fact that the coarser-resolution gridded temperature surfaces are generated by interpolating observations from weather stations that are almost exclusively located in open environments (De Frenne & Verheyen, 2016) and therefore fail to capture the buffering effect of canopies on local temperatures (Figure 6b,d).

This mismatch between readily available gridded climate surfaces and local-scale microclimate observations has major implications for how we model species distributions and up-scale ecosystem processes in the face of global change (De Frenne et al., 2013; Lenoir et al., 2017). As such, generating climate surfaces that are more representative of conditions on the ground is considered by many as a high priority (Bramer et al., 2018; De Frenne & Verheyen, 2016). Encouragingly, our results—along with those of a handful of other studies (e.g., Frey et al., 2016; Lenoir et al., 2017; Tymen et al., 2017)—suggest that 3D remote sensing technologies such as ALS hold real promise in this respect. Looking ahead, as NASA prepares to launch the first spaceborne laser scanner designed specifically to characterize the structure of the world's forest as part of their upcoming GEDI mission (<https://science.nasa.gov/missions/gedi>), we may soon be in a position to radically advance our ability to monitor microclimate on a global scale.

ACKNOWLEDGEMENTS

This work was funded through NERC's Human Modified Tropical Forests Programme (grant number NE/K016377/1 awarded to the BALI consortium) and by the Sime Darby Foundation. D.A.C. was supported by a Leverhulme International Fellowship. We thank NERC's Airborne Research Facility and Data Analysis Node for conducting the airborne survey and preprocessing the data. We acknowledge the Sabah Biodiversity Centre, Sabah Biodiversity Council, Maliau Basin and Danum Valley Management Committees

and the Economic Planning Unit for their support, access to field sites and for permission to carry out fieldwork in Sabah. We also wish to thank the South East Asia Rainforest Research Partnership, Sabah Foundation, Benta Wawasan, the State Secretary, Sabah Chief Minister's Departments and the Sabah Forestry Department. We are grateful to Laura Kruitbos, Unding Jami and the many field assistants who contributed to logistics and data collection. Lastly, we thank three anonymous reviewers for their insightful and constructive comments to our article.

AUTHOR CONTRIBUTION

D.A.C. coordinated the NERC airborne surveys of the SAFE project, which is led by R.M.E.; T.J. and D.A.C. designed the study; T.J., T.S. and D.T.M. processed the airborne imagery; S.R.H., S.B. and D.M.O.E. acquired the microclimate data; T.J. analysed the data and wrote the first draft of the manuscript, with all authors contributing substantially to revisions.

ORCID

Tommaso Jucker  <http://orcid.org/0000-0002-0751-6312>

Sabine Both  <http://orcid.org/0000-0003-4437-5106>

David A. Coomes  <http://orcid.org/0000-0002-8261-2582>

REFERENCES

- Alexander, C., Korstjens, A. H., & Hill, R. A. (2018). Influence of micro-topography and crown characteristics on tree height estimations in tropical forests based on LiDAR canopy height models. *International Journal of Applied Earth Observation and Geoinformation*, 65, 105–113. <https://doi.org/10.1016/j.jag.2017.10.009>
- Anderson, D. B. (1936). Relative humidity or vapor pressure deficit. *Ecology*, 17, 277–282. <https://doi.org/10.2307/1931468>
- Bolton, D. (1980). The computation of equivalent potential temperature. *Monthly Weather Review*, 108, 1046–1053. [https://doi.org/10.1175/1520-0493\(1980\)108aabb1046:TCOEPTaabb2.0.CO;2](https://doi.org/10.1175/1520-0493(1980)108aabb1046:TCOEPTaabb2.0.CO;2)
- Both, S., Elias, D. M. O., Kritzler, U. H., Ostle, N. J., & Johnson, D. (2017). Land use not litter quality is a stronger driver of decomposition in hyperdiverse tropical forest. *Ecology and Evolution*, 7, 9307–9318. <https://doi.org/10.1002/ece3.3460>
- Bradford, M. A., Wieder, W. R., Bonan, G. B., Fierer, N., Raymond, P. A., & Crowther, T. W. (2016). Managing uncertainty in soil carbon feedbacks to climate change. *Nature Climate Change*, 6, 751–758. <https://doi.org/10.1038/nclimate3071>
- Bramer, I., Anderson, B. J., Bennie, J., Bladon, A. J., DeFrenne, P., & Hemming, D. Gillingham, P. K. (2018). Advances in monitoring and modelling climate at ecologically relevant scales. *Advances in Ecological Research*, 58, 101–161.
- Bryan, J. E., Shearman, P. L., Asner, G. P., Knapp, D. E., Aoro, G., & Lokes, B. (2013). Extreme differences in forest degradation in Borneo: Comparing practices in Sarawak, Sabah, and Brunei. *PLoS ONE*, 8, e69679. <https://doi.org/10.1371/journal.pone.0069679>
- Camargo, J. L. C., & Kapos, V. (1995). Complex edge effects on soil moisture and microclimate in central Amazonian forest. *Journal of Tropical Ecology*, 11, 205–221. <https://doi.org/10.1017/S026646740000866X>
- Carey, J. C., Tang, J., Templer, P. H., Kroeger, K. D., Crowther, T. W., Burton, A. J., ... Tietema, A. (2016). Temperature response of soil respiration largely unaltered with experimental warming. *Proceedings of the National Academy of Sciences*, 113, 13797–13802. <https://doi.org/10.1073/pnas.1605365113>
- Chazdon, R. I., Peres, C. a., Dent, D., Sheil, D., Lugo, A. e., Lamb, D., ... Miller, S. e. (2009). The potential for species conservation in tropical secondary forests. *Conservation Biology*, 23, 1406–1417. <https://doi.org/10.1111/j.1523-1739.2009.01338.x>
- Chen, J., Saunders, S. C., Crow, T. R., Naiman, R. J., Brosfokske, K. D., Mroz, G. D., ... Franklin, J. F. (1999). Microclimate in forest ecosystem and landscape ecology. *BioScience*, 49, 288–297. <https://doi.org/10.2307/1313612>
- Clarke, A. (2017). *Principles of thermal ecology: Temperature, energy and life*, Vol. 464 (p. pp.). Oxford, UK: Oxford University Press.
- Coomes, D. A., Šafka, D., Shepherd, J., Dalponte, M., & Holdaway, R. (2018). Airborne laser scanning of natural forests in New Zealand reveals the influences of wind on forest carbon. *Forest Ecosystems*, 5, 1–14.
- De Frenne, P., Rodriguez-Sanchez, F., Coomes, D. a., Baeten, L., Verstraeten, G., Vellend, M., ... Verheyen, K. (2013). Microclimate moderates plant responses to macroclimate warming. *Proceedings of the National Academy of Sciences*, 110, 18561–18565. <https://doi.org/10.1073/pnas.1311190110>
- De Frenne, P., & Verheyen, K. (2016). Weather stations lack forest data. *Science*, 351, 234. <https://doi.org/10.1126/science.351.6270.234-a>
- Deere, N. J., Guillera-Aroita, G., Baking, E. L., Bernard, H., Pfeifer, M., Reynolds, G., ... Struebig, M. J. (2018). High Carbon Stock forests provide co-benefits for tropical biodiversity (ed Magrach A). *Journal of Applied Ecology*, 55, 997–1008. <https://doi.org/10.1111/1365-2664.13023>
- Detto, M., Muller-Landau, H. C., Mascaró, J., & Asner, G. P. (2013). Hydrological networks and associated topographic variation as templates for the spatial organization of tropical forest vegetation. *PLoS ONE*, 8, e76296. <https://doi.org/10.1371/journal.pone.0076296>
- Dobrowski, S. Z. (2011). A climatic basis for microrefugia: The influence of terrain on climate. *Global Change Biology*, 17, 1022–1035. <https://doi.org/10.1111/j.1365-2486.2010.02263.x>
- Doughty, C. E., & Goulden, M. L. (2008). Are tropical forests near a high temperature threshold? *Journal of Geophysical Research*, 113, G00B07. <https://doi.org/10.1029/2007JG000632>
- Duveiller, G., Hooker, J., & Cescatti, A. (2018). The mark of vegetation change on Earth's surface energy balance. *Nature Communications*, 9, 1–12. <https://doi.org/10.1038/s41467-017-02810-8>
- Ehrmann, S., Liira, J., Gärtner, S., Hansen, K., Brunet, J., Cousins, S. A. O., ... Scherer-Lorenzen, M. (2017). Environmental drivers of Ixodes ricinus abundance in forest fragments of rural European landscapes. *BMC Ecology*, 17, 1–14. <https://doi.org/10.1186/s12898-017-0141-0>
- Ewers, R. M., & Banks-Leite, C. (2013). Fragmentation impairs the microclimate buffering effect of tropical forests (ed Bohrer G). *PLoS ONE*, 8, e58093.
- Ewers, R. M., Boyle, M. J. W., Gleave, R. A., Plowman, N. S., Benedick, S., Bernard, H., ... Turner, E. C. (2015). Logging cuts the functional importance of invertebrates in tropical rainforest. *Nature Communications*, 6, 6836. <https://doi.org/10.1038/ncomms7836>
- Ewers, R. M., Didham, R. K., Fahrig, L., Ferraz, G., Hector, A., Holt, R. D., & Turner, E. C. (2011). A large-scale forest fragmentation experiment: The Stability of Altered Forest Ecosystems Project. *Philosophical Transactions of the Royal Society B*, 366, 3292–3302. <https://doi.org/10.1098/rstb.2011.0049>
- Faye, E., Herrera, M., Bellomo, L., & Dangles, O. (2014). Strong discrepancies between local temperature mapping and interpolated climatic grids in tropical mountainous agricultural landscapes. *PLoS ONE*, 9, e105541. <https://doi.org/10.1371/journal.pone.0105541>
- Fick, S. E., & Hijmans, R. J. (2017). WorldClim 2: New 1-km spatial resolution climate surfaces for global land areas. *International Journal of Climatology*, 37, 4302–4315. <https://doi.org/10.1002/joc.5086>

- Frey, S. J. K., Hadley, A. S., Johnson, S. L., Schulze, M., Jones, J. A., & Betts, M. G. (2016). Spatial models reveal the microclimatic buffering capacity of old-growth forests. *Science Advances*, 2, e1501392–e1501392. <https://doi.org/10.1126/sciadv.1501392>
- García-Robledo, C., Kuprewicz, E. K., Staines, C. L., Erwin, T. L., & Kress, W. J. (2016). Limited tolerance by insects to high temperatures across tropical elevational gradients and the implications of global warming for extinction. *Proceedings of the National Academy of Sciences*, 113, 680–685. <https://doi.org/10.1073/pnas.1507681113>
- Gaveau, D. L. A., Sheil, D., Husnayaen, S., Salim, M. A., Arjasakusuma, S., Ancrenaz, M., ... Meijaard, E. (2016). Rapid conversions and avoided deforestation: Examining four decades of industrial plantation expansion in Borneo. *Scientific Reports*, 6, 32017. <https://doi.org/10.1038/srep32017>
- Gaveau, D. L. A., Sloan, S., Molidena, E., Yaen, H., Sheil, D., Abram, N. K., ... Meijaard, E. (2014). Four decades of forest persistence, clearance and logging on Borneo. *PLoS ONE*, 9, e101654. <https://doi.org/10.1371/journal.pone.0101654>
- Graham, V., Laurance, S. G., Grech, A., McGregor, A., & Venter, O. (2016). A comparative assessment of the financial costs and carbon benefits of REDD+ strategies in Southeast Asia. *Environmental Research Letters*, 11, 114022. <https://doi.org/10.1088/1748-9326/11/11/114022>
- Grömping, U. (2006). R package relaimpo: Relative importance for linear regression. *Journal of Statistical Software*, 17, 139–147.
- Hardwick, S. R. (2015). Interactions between vegetation and microclimate in a heterogeneous tropical landscape. *Imperial College London*, 138, pp.
- Hardwick, S. R., Toumi, R., Pfeifer, M., Turner, E. C., Nilus, R., & Ewers, R. M. (2015). The relationship between leaf area index and microclimate in tropical forest and oil palm plantation: Forest disturbance drives changes in microclimate. *Agricultural and Forest Meteorology*, 201, 187–195. <https://doi.org/10.1016/j.agrformet.2014.11.010>
- Hijmans, R. J. (2016). *raster: Geographic data analysis and modeling*. R package version (p. 2.5–8. <https://CRAN.R-project.org/package=raster>).
- Holl, K. D. (1999). Factors limiting tropical rain forest regeneration in abandoned pasture: Seed rain, seed germination, microclimate and soil. *Biotropica*, 31, 229–242.
- IPCC (2014). *IPCC, 2014: Climate Change 2014: Synthesis Report. Contribution of Working Groups I, II and III to the Fifth Assessment Report of the Intergovernmental Panel on Climate Change* (eds Pachauri RK, Meyer LA) (p. 151). Geneva, Switzerland: IPCC.
- Jones, C. D., Cox, P., & Huntingford, C. (2003). Uncertainty in climate-carbon-cycle projections associated with the sensitivity of soil respiration to temperature. *Tellus Series B*, 55, 642–648. <https://doi.org/10.1034/j.1600-0889.2003.01440.x>
- Jucker, T., Asner, G. P., Dalponte, M., et al. (2018). Estimating above-ground carbon density and its uncertainty in Borneo's structurally complex tropical forests using airborne laser scanning. *Biogeosciences*, 15, 3811–3830.
- Jucker, T., Bongalov, B., Burslem, D. F. R. P., et al. (2018). Topography shapes the structure, composition and function of tropical forest landscapes. *Ecology Letters*, 21, 989–1000.
- Kaspari, M., Clay, N. A., Lucas, J., Yanoviak, S. P., & Kay, A. (2015). Thermal adaptation generates a diversity of thermal limits in a rainforest ant community. *Global Change Biology*, 21, 1092–1102. <https://doi.org/10.1111/gcb.12750>
- Khosravipour, A., Skidmore, A. K., Isenburg, M., Wang, T., & Hussin, Y. A. (2014). Generating pit-free canopy height models from airborne LiDAR. *Photogrammetric Engineering & Remote Sensing*, 80, 863–872. <https://doi.org/10.14358/PERS.80.9.863>
- King, D. A., Davies, S. J., Tan, S., & Nur Supardi, M. N. (2009). Trees approach gravitational limits to height in tall lowland forests of Malaysia. *Functional Ecology*, 23, 284–291. <https://doi.org/10.1111/j.1365-2435.2008.01514.x>
- Labrière, N., Locatelli, B., Laumonier, Y., Freycon, V., & Bernoux, M. (2015). Soil erosion in the humid tropics: A systematic quantitative review. *Agriculture, Ecosystems & Environment*, 203, 127–139. <https://doi.org/10.1016/j.agee.2015.01.027>
- Lefcheck, J. S. (2016). piecewiseSEM: Piecewise structural equation modelling in R for ecology, evolution, and systematics. *Methods in Ecology and Evolution*, 7, 573–579.
- Lefsky, M. A., Cohen, W. B., Parker, G. G., & Harding, D. J. (2002). Lidar remote sensing for ecosystem studies. *BioScience*, 52, 19–30. [https://doi.org/10.1641/0006-3568\(2002\)052\[0019:LRSFES\]2.0.CO;2](https://doi.org/10.1641/0006-3568(2002)052[0019:LRSFES]2.0.CO;2)
- Lenoir, J., Hattab, T., & Pierre, G. (2017). Climatic microrefugia under anthropogenic climate change: Implications for species redistribution. *Ecography*, 40, 253–266. <https://doi.org/10.1111/ecog.02788>
- Lindeman, R. H., Merenda, P. F., & Gold, R. Z. (1980). *Introduction to bivariate and multivariate analysis* (p. 444). Foresman, Glenview: Scott.
- Martin, P. A., Newton, A. C., & Bullock, J. M. (2013). Carbon pools recover more quickly than plant biodiversity in tropical secondary forests. *Proceedings of the Royal Society B: Biological Sciences*, 280, 20132236–20132236. <https://doi.org/10.1098/rspb.2013.2236>
- McAlpine, C. A., Johnson, A., Salazar, A., Syktus, J., Wilson, K., Meijaard, E., ... Sheil, D. (2018). Forest loss and Borneo's climate. *Environmental Research Letters*. <https://doi.org/10.1088/1748-9326/aaa4ff>
- McDowell, N., Allen, C. D., Anderson-Teixeira, K., Brando, P., Brienen, R., Chambers, J., ... Xu, X. (2018). Drivers and mechanisms of tree mortality in moist tropical forests. *New Phytologist*, 219, 851–869. <https://doi.org/10.1111/nph.15027>
- Minder, J. R., Mote, P. W., & Lundquist, J. D. (2010). Surface temperature lapse rates over complex terrain: Lessons from the Cascade Mountains. *Journal of Geophysical Research Atmospheres*, 115, 1–13. <https://doi.org/10.1029/2009JD013493>
- Motzer, T., Munz, N., Kupperts, M., Schmitt, D., & Anhu, D. (2005). Stomatal conductance, transpiration and sap flow of tropical montane rain forest trees in the southern Ecuadorian Andes. *Tree Physiology*, 25, 1283–1293. <https://doi.org/10.1093/treephys/25.10.1283>
- Pfeifer, M., Kor, L., Nilus, R., Turner, E., Cusack, J., Lysenko, I., ... Ewers, R. M. (2016). Mapping the structure of Borneo's tropical forests across a degradation gradient. *Remote Sensing of Environment*, 176, 84–97. <https://doi.org/10.1016/j.rse.2016.01.014>
- Poorter, L., Bongers, F., Aide, T. M., Almeyda Zambrano, A. M., Balvanera, P., Becknell, J. M., ... Rozendaal, D. M. A. (2016). Biomass resilience of Neotropical secondary forests. *Nature*, 530, 211–214. <https://doi.org/10.1038/nature16512>
- Potter, K. A., Arthur Woods, H., & Pincebourde, S. (2013). Microclimatic challenges in global change biology. *Global Change Biology*, 19, 2932–2939. <https://doi.org/10.1111/gcb.12257>
- R Core Development Team. (2016). *R: A language and environment for statistical computing*. Vienna, Austria: R Foundation for Statistical Computing.
- Riutta, T., Malhi, Y., Kho, L. K., Marthews, T. R., Huaraca Huasco, W., Khoo, M. S., ... Ewers, R. M. (2018). Logging disturbance shifts net primary productivity and its allocation in Bornean tropical forests. *Global Change Biology*, 24, 2913–2928. <https://doi.org/10.1111/gcb.14068>
- Sanginés de Cárcer, P., Vitasse, Y., Peñuelas, J., Jassey, V. E. J., Buttler, A., & Signarbieux, C. (2018). Vapor-pressure deficit and extreme climatic variables limit tree growth. *Global Change Biology*, 24, 1108–1122. <https://doi.org/10.1111/gcb.13973>
- Scheffers, B. R., Edwards, D. P., Macdonald, S. L., Senior, R. A., Andriamahohatra, L. R., Roslan, N., ... Williams, S. E. (2017). Extreme thermal heterogeneity in structurally complex tropical rain forests. *Biotropica*, 49, 35–44. <https://doi.org/10.1111/btp.12355>

- Scriven, S. A., Hodgson, J. A., McClean, C. J., & Hill, J. K. (2015). Protected areas in Borneo may fail to conserve tropical forest biodiversity under climate change. *Biological Conservation*, 184, 414–423. <https://doi.org/10.1016/j.biocon.2015.02.018>
- Senior, R. A., Hill, J. K., Benedick, S., & Edwards, D. P. (2017). Tropical forests are thermally buffered despite intensive selective logging. *Global Change Biology*, 24, 1267–1278. <https://doi.org/10.1111/gcb.13914>
- Senior, R. A., Hill, J. K., González del Pliego, P., Goode, L. K., & Edwards, D. P. (2017). A pantropical analysis of the impacts of forest degradation and conversion on local temperature. *Ecology and Evolution*, 7, 7897–7908. <https://doi.org/10.1002/ece3.3262>
- Sidle, R. C., Ziegler, A. D., Negishi, J. N., Rahim, A., Siew, R., & Turkelboom, F. (2006). Erosion processes in steep terrain — truths, myths, and uncertainties related to forest management in Southeast Asia. *Forest Ecology and Management*, 224, 199–225. <https://doi.org/10.1016/j.foreco.2005.12.019>
- Smith, J. M. B. (1977). Vegetation and microclimate of east- and west-facing slopes in the grasslands of MT Wilhelm, Papua New Guinea. *Journal of Ecology*, 65, 39–53. <https://doi.org/10.2307/2259061>
- Stark, S. C., Leitold, V., Wu, J. L., Hunter, M. O., de Castilho, C. V., Costa, F. R. C., ... Saleska, S. R. (2012). Amazon forest carbon dynamics predicted by profiles of canopy leaf area and light environment. *Ecology Letters*, 15, 1406–1414. <https://doi.org/10.1111/j.1461-0248.2012.01864.x>
- Sunday, J. M., Bates, A. E., & Dulvy, N. K. (2011). Global analysis of thermal tolerance and latitude in ectotherms. *Philosophical Transactions of the Royal Society B: Biological Sciences*, 278, 1823–1830. <https://doi.org/10.1098/rspb.2010.1295>
- Swetnam, T. L., Brooks, P. D., Barnard, H. R., Harpold, A. A., & Gallo, E. L. (2017). Topographically driven differences in energy and water constrain climatic control on forest carbon sequestration. *Ecosphere*, 8, e01797. <https://doi.org/10.1002/ecs2.1797>
- Tan, Z.-H., Zeng, J., Zhang, Y.-J., Slot, M., Gamo, M., Hirano, T., ... Restrepo-Coupe, N. (2017). Optimum air temperature for tropical forest photosynthesis: Mechanisms involved and implications for climate warming. *Environmental Research Letters*, 12, 054022. <https://doi.org/10.1088/1748-9326/aa6f97>
- Thirumalai, K., DiNezio, P. N., Okumura, Y., & Deser, C. (2017). Extreme temperatures in Southeast Asia caused by El Niño and worsened by global warming. *Nature Communications*, 8, 15531. <https://doi.org/10.1038/ncomms15531>
- Tymen, B., Vincent, G., Courtois, E. A., Heurtebize, J., Dauzat, J., Marechaux, I., & Chave, J. (2017). Quantifying micro-environmental variation in tropical rainforest understory at landscape scale by combining airborne LiDAR scanning and a sensor network. *Annals of Forest Science*, 74(2), <https://doi.org/10.1007/s13595-017-0628-z>
- Walsh, R. P. D., & Newbery, D. M. (1999). The ecoclimatology of Danum, Sabah, in the context of the world's rainforest regions, with particular reference to dry periods and their impact. *Philosophical Transactions of the Royal Society B*, 354, 1869–1883. <https://doi.org/10.1098/rstb.1999.0528>
- Way, D. A., & Oren, R. (2010). Differential responses to changes in growth temperature between trees from different functional groups and biomes: A review and synthesis of data. *Tree Physiology*, 30, 669–688. <https://doi.org/10.1093/treephys/tpq015>
- Werner, F. A., & Homeier, J. (2015). Is tropical montane forest heterogeneity promoted by a resource-driven feedback cycle? Evidence from nutrient relations, herbivory and litter decomposition along a topographical gradient. *Functional Ecology*, 29, 430–440. <https://doi.org/10.1111/1365-2435.12351>
- Will, R. E., Wilson, S. M., Zou, C. B., & Hennessey, T. C. (2013). Increased vapor pressure deficit due to higher temperature leads to greater transpiration and faster mortality during drought for tree seedlings common to the forest-grassland ecotone. *New Phytologist*, 200, 366–374. <https://doi.org/10.1111/nph.12321>
- Wulder, M. A., White, J. C., Nelson, R. F., Næsset, E., Ørka, H. O., Coops, N. C., ... Gobakken, T. (2012). Lidar sampling for large-area forest characterization: A review. *Remote Sensing of Environment*, 121, 196–209. <https://doi.org/10.1016/j.rse.2012.02.001>

SUPPORTING INFORMATION

Additional supporting information may be found online in the Supporting Information section at the end of the article.

How to cite this article: Jucker T, Hardwick SR, Both S, et al. Canopy structure and topography jointly constrain the microclimate of human-modified tropical landscapes. *Glob Change Biol*. 2018;24:5243–5258. <https://doi.org/10.1111/gcb.14415>